

Energy Efficiency of RSMA and NOMA in Cellular-Connected mmWave UAV Networks

Ali Rahmati*, Yavuz Yapıcı*, Nadisanka Rupasinghe*, İsmail Güvenç*, Huaiyu Dai*, and Arupjyoti Bhuyan†

*Dept. of Electrical and Computer Engineering, North Carolina State University, Raleigh, NC

†Idaho National Laboratory, Idaho Falls, ID

Email:{arahmat, yyapici, rrupasi, iguven, hdai}@ncsu.edu, arupjyoti.bhuyan@inl.gov

Abstract—Cellular-connected unmanned aerial vehicles (UAVs) are recently getting significant attention due to various practical use cases, e.g., surveillance, data gathering, purchase delivery, among other applications. Since UAVs are low power nodes, energy and spectral efficient communication is of paramount importance. To that end, multiple access (MA) schemes can play an important role in achieving high energy efficiency and spectral efficiency. In this work, we introduce rate-splitting MA (RSMA) and non-orthogonal MA (NOMA) schemes in a cellular-connected UAV network. In particular, we investigate the energy efficiency of the RSMA and NOMA schemes in a millimeter-wave (mmWave) downlink transmission scenario. Furthermore, we optimize precoding vectors of both the schemes by explicitly taking into account the 3GPP antenna propagation patterns. The numerical results for this realistic transmission scheme indicate that RSMA is superior to NOMA in terms of overall energy efficiency.

Index Terms—3GPP, antenna propagation patterns, cellular-connected, energy efficiency, mmWave, NOMA, RSMA, UAVs.

I. INTRODUCTION

The use of unmanned aerial vehicles (UAVs) in wireless networks is considered a key component of next generation communications systems [1]–[3]. Beside improving the network coverage through broadband mobile data delivery, UAVs have already become one of the major building blocks of various applications involving public safety, disaster relief, and surveillance, to name a few. In order to speed up deployment of UAVs in communications scenarios, one common approach is to employ UAVs as an integral part of the terrestrial wireless networks. By this way, infrastructure costs associated with serving flying UAVs are aimed to decrease as much as possible by making use of the existing network capabilities.

In the *cellular-connected UAV* concept, existing terrestrial wireless networks serve flying UAVs while their primary users are placed on the ground. The terrestrial BSs therefore have long-term relatively static features (e.g., down-tilted transmit antenna arrays) which are optimized considering ground users. The propagation pattern can, however, be *shaped* taking into account not only the ground users but also the desired UAVs through advanced beamforming techniques. A more viable approach in simultaneously serving UAVs and ground users

is to use state-of-the-art multiple access (MA) transmission schemes. By adequately allocating available resources (e.g., power, time-frequency slots), the interference that arises when serving multiple users simultaneously can be handled effectively through novel MA techniques.

Non-orthogonal MA (NOMA) is identified as a promising MA scheme for 5G and beyond cellular communication technologies which can also be a smart solution for cellular-connected UAV scenarios [4], [5]. The NOMA transmission enables serving multiple UAVs at the same time, frequency and space resources enhancing the spectral efficiency. However, NOMA may not be the optimal MA scheme for multiple-input single-output (MISO) broadcast channels, except under overloaded conditions (i.e., user channels are highly correlated and not orthogonal). Moreover, the optimal user pairing and decoding order are two main drawbacks of the NOMA strategy in practical applications, which increase the system complexity. Space division MA (SDMA) on the other hand is more suitable for underloaded conditions which however achieves degraded performance when network load is high. Recently, rate splitting MA (RSMA) is receiving significant attention as an effective MA scheme for next generation wireless communication systems. RSMA is preferable irrespective of the loading condition. In fact, RSMA enables soft bridging between two extremes, NOMA and SDMA [6].

In this work, we investigate the energy efficiency of various MA schemes in a downlink mmWave cellular-connected UAV network. In particular, we consider RSMA and NOMA as two MA schemes of interest, and optimize each scheme to maximize the energy efficiency. Furthermore, we assume that the BS serving the desired UAVs actually belongs to a next generation terrestrial wireless network, and that the transmit antenna array is therefore composed of antenna elements having 3GPP propagation patterns. To the best of our knowledge, this is the first time that the energy efficiency of MA schemes are being studied in the context of cellular-connected mmWave UAV network with realistic propagation patterns. The numerical results verify the superiority of RSMA to NOMA in terms of energy efficiency in different scenarios.

The rest of the paper is organized as follows. In Section II, the system model along with mmWave channel model and 3GPP antenna patterns are presented. The MA schemes are considered in Section III together with exact energy efficiency

This work is supported in part through the INL Laboratory Directed Research & Development (LDRD) Program under DOE Idaho Operations Office Contract DE-AC07-05ID14517.

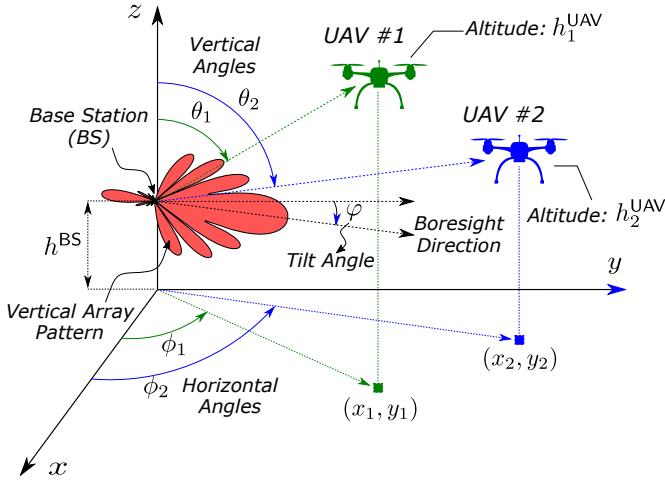


Figure 1: System model for mmWave downlink serving cellular-connected UAVs simultaneously. The vertical propagation pattern of the 8-element antenna array is also illustrated.

optimization for RSMA and NOMA techniques involving 3GPP antenna patterns. Section IV presents numerical results on the performance of the considered schemes, and Section V finally concludes the paper.

II. SYSTEM MODEL

In this section, we overview the downlink communication scenario involving UAVs as user terminals, mmWave channel model, and 3GPP antenna pattern considered in this work.

A. Scenario Description

We consider a downlink transmission scenario in a single cell of a mmWave communications network. We assume that a conventional BS is responsible for serving desired ground users, and is therefore tilted downwards by an angle φ , as shown in Fig. 1. The transmit antenna structure at the BS is composed of a uniform linear array (ULA) with M identical antenna elements placed vertically (i.e., along z -axis in Fig. 1) [7], [8]. In our specific setting, we focus our attention to the downlink transmission where the BS is serving UAVs flying at various altitudes (i.e., *cellular-connected UAVs*). Since the BS antenna array is configured to point downwards, the UAVs are assumed to be served using not only the main lobe but also the side lobes of the ULA propagation pattern depending on the altitude.

We assume that the terrestrial BS, which is off the ground vertically by h^{BS} , is assigned a number of K flying UAVs at altitudes h_k^{UAV} with the projection points (x_k, y_k) on the xy -plane for $k \in \{1, \dots, K\}$. The BS aims to transmit dedicated messages to each UAV simultaneously (i.e., using the same time-frequency resources), where the message for the k th UAV is denoted by W_k . These messages are precoded based on various MA schemes, and form the composite transmit signal $\mathbf{x} \in \mathbb{C}^{M \times 1}$. We assume that the total transmit power at the BS is subject to a power constraint P_t given as $\mathbb{E}\{\|\mathbf{x}\|^2\} \leq P_t$.

B. mmWave Channel Model

We assume a mmWave downlink transmission with \mathbf{h}_k being the channel between the BS and the k th UAV, which is given as [9]–[11]

$$\mathbf{h}_k = \sqrt{M} \sum_{p=1}^{N_p} \frac{\alpha_{k,p} \mathbf{a}(\theta_{k,p})}{\left[\text{PL} \left(\sqrt{d_k^2 + (\Delta h_k^{\text{UAV}})^2} \right) \right]^{1/2}}, \quad (1)$$

where N_p is the number of multipaths, $\alpha_{k,p}$ is the gain of the p th following standard complex Gaussian distribution, $\theta_{k,p}$ is the angle-of-departure (AoD) of the p th path. Furthermore, $\Delta h_k^{\text{UAV}} = h_k^{\text{UAV}} - h^{\text{BS}}$ describes the relative altitude of the k th UAV (i.e., vertical distance with respect to the BS) assuming $h_k^{\text{UAV}} > h^{\text{BS}}$, and $d_k = \sqrt{x_k^2 + y_k^2}$ stands for the ground distance of the k th UAV on the xy -plane (i.e., horizontal distance with respect to the BS). In addition, PL represents the path loss of the downlink channel, which is described for the k th UAV using the line-of-sight (LoS) distance with respect to the BS.

In (1), $\mathbf{a}(\theta_{k,p})$ is the array steering vector, which is

$$\left[\mathbf{a}(\theta_{k,p}) \right]_i = \exp \left\{ -j2\pi \frac{D}{\lambda} (i-1) \cos(\theta_{k,p}) \right\}, \quad (2)$$

for $i = 1, \dots, M$ with $[\cdot]_i$ denoting the i th entry, where D is the antenna element spacing along ULA, and λ is the wavelength of the carrier frequency. We also assume that each UAVs has LoS path to the BS owing to sufficiently high flying altitudes, and the fact that probability of having scatters around any UAV is very small. Considering the well-known characteristic of the mmWave transmission where LoS path is significantly dominant as compared to the Non-LoS (NLoS) paths, we assume a single LoS path for the channel under consideration, and (1) accordingly becomes [4]

$$\mathbf{h}_k = \sqrt{M} \frac{\alpha_k \mathbf{a}(\theta_k)}{\left[\text{PL} \left(\sqrt{d_k^2 + (\Delta h_k^{\text{UAV}})^2} \right) \right]^{1/2}}, \quad (3)$$

where θ_k is the AoD of the LoS path.

C. Impact of 3GPP Antenna Pattern

In the cellular-connected UAV scenario considered in our study, we assume that the transmit antenna array at the terrestrial BS is physically tilted downwards to serve the primary users of the existing network on the ground (i.e., see the angle φ in Fig. 1). The desired UAVs are therefore served by not only the main lobe but also the side lobes of the antenna array propagation pattern [12]. Hence, the specific pattern of the array antennas in the vertical domain plays a crucial role in the overall network performance. In our study, we adopt 3GPP realistic antenna pattern [7], [8], [13], and present how to incorporate this model into our setting in the following.

In order to weigh the transmission using the propagation pattern at the BS, we need to determine the vertical and horizontal angles θ and ϕ , respectively. Considering the

engagement geometry depicted in Fig. 1, the vertical angle for the k th UAV can be given as

$$\theta_k = \frac{\pi}{2} - \tan^{-1} \left(\frac{\Delta h_k^{\text{UAV}}}{d_k} \right), \quad (4)$$

and the horizontal angle is similarly given as

$$\phi_k = \tan^{-1} \left(\frac{y_k}{x_k} \right). \quad (5)$$

Considering 3GPP model [8], [14], radiation pattern of the single antenna element in the vertical domain is given as

$$A_{E,H}(\theta, \varphi) = -\min \left\{ 12 \left(\frac{\theta - 90 - \varphi}{\theta_{3\text{dB}}} \right)^2, SLA_V \right\}, \quad (6)$$

where $\theta_{3\text{dB}} = 65^\circ$ is the 3-dB vertical beamwidth, $SLA_V = 30$ dB is the side lobe level limit (i.e., side lobes away from the main lobe by greater than SLA_V is discarded), and φ is the vertical tilt angle depicted in Fig. 1. Similarly, the horizontal pattern of the single antenna element is given as

$$A_{E,H}(\phi) = -\min \left\{ 12 \left(\frac{\phi}{\phi_{3\text{dB}}} \right)^2, A_m \right\}, \quad (7)$$

where $\phi_{3\text{dB}} = 65^\circ$ is the 3-dB horizontal beamwidth, and $A_m = 30$ dB is the front-back ratio (i.e., the gain difference between the back and main lobes). Combining (6) and (7), the 3D antenna element propagation pattern for the angle pair (θ, ϕ) is given as

$$A_E(\theta, \phi) = G_{\text{max}} - \min \left\{ -[A_{E,V}(\theta, \varphi) + A_{E,H}(\phi)], A_m \right\} \quad (8)$$

where G_{max} is the maximum directional gain of the antenna element in the transmit antenna array. We note that (8) stands for only the antenna element propagation pattern adopting 3GPP model, and therefore does not consider any contribution from array gain. The gain G_k in (1) can then be given as $G_k = A_E(\theta_k, \phi_k)$ where the angle pair θ_k and ϕ_k for the k th UAV are given in (4) and (5), respectively. It should be noted that $A_E(\theta_k, \phi_k)$ is in dB but needs to be converted to linear scale.

III. MULTIPLE ACCESS FOR CELLULAR-CONNECTED UAVS

In this section, we consider two MA schemes (i.e, RSMA and NOMA) to serve several cellular-connected UAVs simultaneously, and optimize the both schemes for energy efficiency considering the user rates and the total power required. In our derivations, we explicitly consider the realistic antenna pattern of 3GPP along with the specific engagement geometry.

A. Rate Splitting Multiple Access (RSMA)

The RSMA strategy is pioneered by [15], where it is shown that the achievable rate region obtained through successive interference cancellation (SIC) is just a fraction of its complete capacity region. In order to produce any rates in the capacity region as much as possible, the RSMA approach is proposed for MA scenarios. In this approach, instead of assigning message of

each user to separate data streams, RSMA suggests to transmit a “common” part of all user messages jointly, and the rest of each user message through different streams called “private”. At the receiver side, each user is expected to decode first the common message (in the presence of all private messages), cancel the effect of this common message from the received signal, and decode its own private message (in the presence of the other private messages).

We assume that the BS encodes part of each stream to be transmitted to a particular UAV as the *common message*, denoted by s_c . The rest of the stream for each UAV is then considered as *private message*, and is encoded into stream s_k for the k th UAV. In order to mitigate the interference as much as possible, we consider different beamforming vectors for each private message as well as the common message. Assuming that \mathbf{w}_k and \mathbf{w}_c represent the beamforming vectors for the private message of the k th UAV and the common message, respectively, the overall beamforming matrix can be given as $\mathbf{W} = [\mathbf{w}_c \mathbf{w}_1 \dots \mathbf{w}_K]$. In addition, the transmit signal at the BS after precoding is given as $\mathbf{x} = \mathbf{W}\mathbf{s}$ where $\mathbf{s} = [s_c s_1 \dots s_K]$ is the overall message vector.

The received signal at the k th UAV is given by:

$$y_k = \sqrt{G_k} \mathbf{h}_k^H \mathbf{W}\mathbf{s} + n_k, \quad (9)$$

$$= \sqrt{G_k} \mathbf{h}_k^H \mathbf{w}_c s_c + \sqrt{G_k} \sum_{\ell=1}^K \mathbf{h}_k^H \mathbf{w}_\ell s_\ell + n_k, \quad (10)$$

where G_k is the gain of the antenna element propagation pattern, $\mathbf{h}_k^H \in \mathbb{C}^{M \times 1}$ is the channel from the BS to the k th UAV, which is assumed to be known perfectly at the BS in our study, and n_k is the circularly symmetric complex Gaussian white noise with zero-mean and variance N_0 , i.e., $n_k \sim \mathcal{CN}(0, N_0)$. Assuming unit-energy message vector \mathbf{s} , the power budget at the BS requires $\text{tr}(\mathbf{W}\mathbf{W}^H) \leq P_t$, which needs to be handled properly in the optimization problem.

In order to decode the entire message for each UAV, the common message has to be decoded first in the presence of the private messages of *all* the UAVs, and then cancel its effect from the received symbol, which is known as successive interference cancellation (SIC). Assuming that common message is successfully decoded in all the UAVs, each UAV then decodes its own private message treating the other private messages as noise. The SINR of the k th UAV while decoding the common message s_c is given as

$$\text{SINR}_k^c = \frac{G_k |\mathbf{h}_k^H \mathbf{w}_c|^2}{G_k \sum_{\ell=1}^K |\mathbf{h}_k^H \mathbf{w}_\ell|^2 + N_0}, \quad (11)$$

and the respective rate (normalized by transmission bandwidth) is expressed as $R_k^c = \log_2(1 + \text{SINR}_k^c)$. We note that the overall success of the decoding process involves private message as well as common message being decoded without any error *at each* UAV. The necessary condition for successful decoding of the common message is that the respective common rate r_k^c for the k th UAV should be less than $R^c = \min\{R_1^c, \dots, R_K^c\}$.

After successfully decoding the common message, and

cancelling its contribution from the received signal, each UAV can decode its own private message in the presence of the other private messages. The respective SINR for the k th UAV is

$$\text{SINR}_k^{\text{P}} = \frac{G_k |\mathbf{h}_k^H \mathbf{w}_k|^2}{G_k \sum_{\ell \neq k} |\mathbf{h}_k^H \mathbf{w}_\ell|^2 + N_0}, \quad (12)$$

and the normalized rate is $R_k^{\text{P}} = \log_2(1 + \text{SINR}_k^{\text{P}})$.

In this study, we optimize the precoding matrix \mathbf{W} and the common rate vector $\mathbf{r}^{\text{c}} = [r_1^{\text{c}} \dots r_K^{\text{c}}]$ to maximize the energy efficiency, which is given for the k th UAV as

$$\text{EE}_k^{\text{RSMA}} = \frac{\beta_k (r_k^{\text{c}} + R_k^{\text{P}})}{\text{tr}(\mathbf{W}\mathbf{W}^H) + P_{\text{BS}}}, \quad (13)$$

where P_{BS} is the fixed power consumption to operate the BS (even without RF transmission), and β_k is the communication-dependent weight factor which might be used to prioritize UAVs based on their quality-of-service (QoS) requirements. The energy efficiency for the overall network is

$$\text{EE}^{\text{RSMA}} = \sum_{k=1}^K \text{EE}_k^{\text{RSMA}}, \quad (14)$$

and the respective optimization problem is given as

$$\max_{\mathbf{r}^{\text{c}}, \mathbf{W}} \text{EE}^{\text{RSMA}} \quad (15)$$

$$\text{s.t.} \quad \text{tr}(\mathbf{W}\mathbf{W}^H) \leq P_t, \quad (15a)$$

$$\sum_{\ell=1}^K r_\ell^{\text{c}} \leq R_k^{\text{c}} \quad \forall k \in \{1, \dots, K\}, \quad (15b)$$

$$\mathbf{r}^{\text{c}} \geq \mathbf{0}, \quad (15c)$$

where the optimization runs over both the common message rate vector \mathbf{r}^{c} as well as the beamforming matrix \mathbf{W} .

B. Non-Orthogonal Multiple Access (NOMA)

The NOMA strategy relies on the fact that user messages are *distinct* enough in the power domain, and each receiver can decode its desired message using the SIC approach. To this end, the NOMA transmitter allocates adequate power to each UAV's message, which requires the knowledge of the channel condition for each UAV. Without any loss of generality, the UAVs with indices from $\mathcal{N} = \{1, \dots, K\}$ are ordered from the one allocated less power to the one allocated more power, and that BS has this information perfectly. Although the power allocation is jointly optimized in the sequel along with the beamforming matrix \mathbf{W} , it is worth noting that the NOMA strategy proceeds with allocating less power to the UAVs having better channel conditions, and vice versa.

Assuming that \mathbf{w}_k is the beamforming vector for the k th UAV, the transmit signal at the BS after precoding is given as $\mathbf{x} = \mathbf{W}\mathbf{s}$ where $\mathbf{W} = [\mathbf{w}_1 \dots \mathbf{w}_K]$. The received signal at the k th UAV now becomes

$$y_k = \sqrt{G_k} \mathbf{h}_k^H \mathbf{W}\mathbf{s} + n_k = \sqrt{G_k} \sum_{\ell=1}^K \mathbf{h}_k^H \mathbf{w}_\ell s_\ell + n_k. \quad (16)$$

In the NOMA strategy, k th UAV is expected to first decode messages of the other UAVs allocated more power (i.e., with the index $m > k$). This decoding is performed by treating the UAVs allocated less power (i.e., with the index $m < k$) as noise. Each decoded message is then subtracted from the received signal in (16) through SIC, and k th UAV finally decodes its own message s_k . In this approach, the SINR associated with decoding the message of the m th UAV (at the k th UAV with $m \geq k$) is given as

$$\text{SINR}_{m \rightarrow k} = \frac{G_k |\mathbf{h}_k^H \mathbf{w}_m|^2}{G_k \sum_{l < m, l \in \mathcal{N}} |\mathbf{h}_k^H \mathbf{w}_l|^2 + N_0}, \quad (17)$$

which implicitly assumes that messages of all the UAVs with the indices greater than m have been decoded successfully and canceled beforehand. Actually, (17) represents the SINR of the k th UAV while decoding its own message (i.e., for $m = k$), as well. Note that the summation in the denominator of (17) disappears when the k th UAV with $k = 1$ is decoding its own message (i.e., no possible l index satisfying $l < k$ for this specific case), and we have $\frac{G_k}{N_0} |\mathbf{h}_k^H \mathbf{w}_k|^2$.

Finally, the normalized rate associated with the k th UAV is

$$R_k = \log_2(1 + \min\{\text{SINR}_{k \rightarrow 1}, \dots, \text{SINR}_{k \rightarrow k}\}). \quad (18)$$

The energy efficiency for the k th UAV is

$$\text{EE}_k^{\text{NOMA}} = \frac{\beta_k R_k}{\text{tr}(\mathbf{W}\mathbf{W}^H) + P_{\text{BS}}}, \quad (19)$$

and for the overall network is

$$\text{EE}^{\text{NOMA}} = \sum_{k=1}^K \text{EE}_k^{\text{NOMA}}. \quad (20)$$

The respective optimization problem therefore becomes

$$\max_{\mathbf{r}^{\text{c}}, \mathbf{W}} \text{EE}^{\text{NOMA}} \quad (21)$$

$$\text{s.t.} \quad \text{tr}(\mathbf{W}\mathbf{W}^H) \leq P_t. \quad (21a)$$

C. Successive Convex Approximation (SCA)

The energy efficiency optimization problems for RSMA and NOMA given by (14) and (20), respectively, are highly non-convex. Thus, we need to come up with an approximate algorithm to solve these optimization problems efficiently. As in [16], we adopt the SCA algorithm [17] as a good match for this problem. The algorithm proposes to approximate the non-convex objective function (or the functions in the constraints) using the first-order Taylor expansion around a given initial point. By this way, the problem is converted to a convex optimization problem, and can therefore be solved efficiently using standard optimization toolboxes (e.g., CVX [18], YALMIP [19]). The algorithm proceeds through iterations such that the optimal values of the variables in the first iteration are employed as the initial values for the next iteration. This procedure is repeated until the convergence is achieved.

Table I: Simulation Parameters

Parameter	Value
Path loss exponent (γ)	2
BS height (h^{BS})	10 m
UAV altitude ($h_1^{\text{UAV}}, h_2^{\text{UAV}}$)	10 – 60 m
BS array size (M)	8
Noise variance (N_0)	1
Total transmit power (P_t)	40 dBm
Weight of 1st UAV (β_1)	1
Weight of 2nd UAV (β_2)	$10^\eta, \eta \in [-2, 2]$
Circuit power consumption (P_c)	40 dBm
Tilt angle (φ)	12°
Maximum directional gain (G_{max})	8 dBi

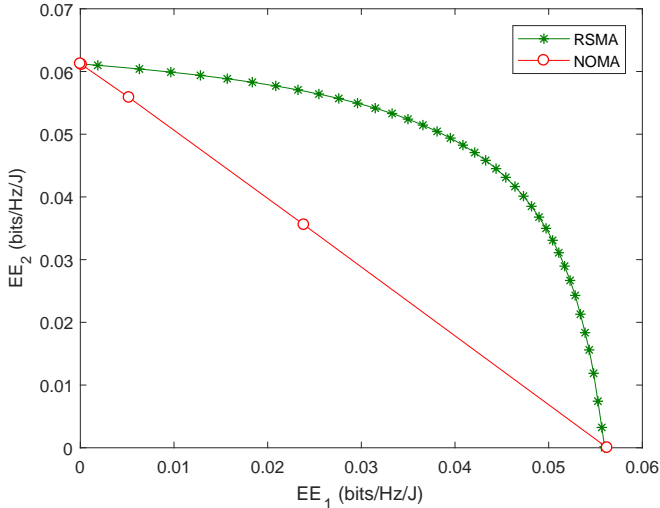


Figure 2: Energy efficiency region for RSMA and NOMA.

IV. SIMULATION RESULTS

In this section, we present numerical results for the performance of RSMA and NOMA considering a downlink mmWave network with 2 cellular-connected UAVs. We adopt the path loss model in [10], [11] with $\text{PL}(x_k) = 1 + x_k^\gamma$, where γ is the path loss exponent, and x_k is the LoS distance between the BS and the k th UAV. We assume that the antenna array of the BS has $M = 8$ elements, which are placed vertically. We assume that the UAVs are fixed in xy -plane during the simulation. The specific simulation parameters are listed in Table I.

In Fig. 2, we depict the energy efficiency region of the 2 cellular-connected UAVs, where the weight factor of the 1st UAV is fixed as $\beta_1 = 1$, and that of the 2nd UAV is varying as $\beta_2 = 10^\eta$ with $\eta \in [-2, 2]$. We furthermore assume a geometry for the model of Fig. 1 for which the locations of the UAVs on the ground are given by the horizontal distances $d_1 = 25$ m and $d_2 = 30$ m, and angles $\phi_1 = \pi/10$, and $\phi_2 = 2\pi/5$. In

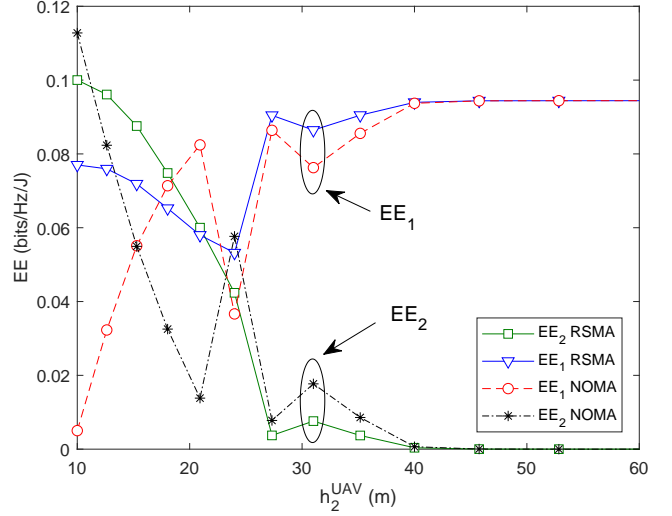


Figure 3: Energy efficiency of each UAV versus the altitude of the 2nd UAV.

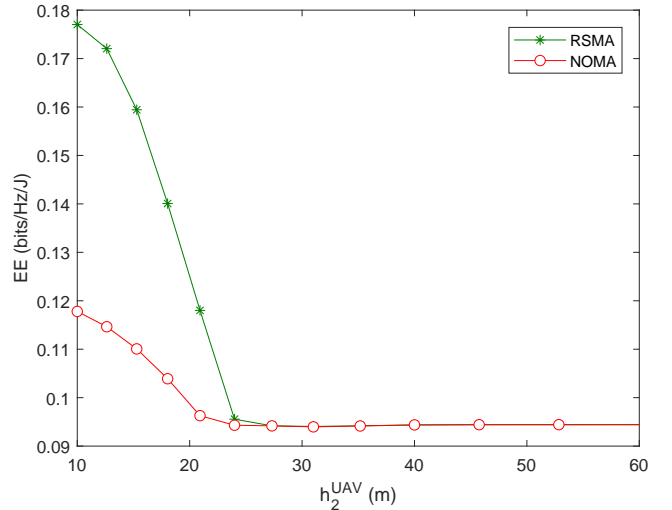


Figure 4: Sum energy efficiency versus the altitude of the 2nd UAV.

addition, altitudes of the UAVs are given as $h_1^{\text{UAV}} = 24.4$ m and $h_2^{\text{UAV}} = 15.3$ m, which correspond to the vertical angles $\theta_1 = \pi/3$ and $\theta_2 = 4\pi/9$ by (4). We observe in Fig. 2 that the energy efficiency of the UAVs with RSMA is superior to that for NOMA for any choice of weight factor β_2 .

In Fig. 3, we demonstrate the energy efficiency of each UAV along with varying altitude of the 2nd UAV such that $h_2^{\text{UAV}} \in [0, 60]$ m. To this end, we keep the simulation parameters of Fig. 2 the same for this experiment except h_2^{UAV} , which requires the vertical angle to vary as $\theta_2 \in [\pi/18, \pi/2]$ by (4). The sum energy efficiency given by (14) and (20) are also depicted in Fig. 4. We observe that the energy efficiency of the 2nd UAV exhibits a decaying trend for both RSMA and NOMA, since it is not reasonable to allocate more power to the 2nd UAV as its altitude gets larger, and, hence, the respective channel degrades along with increasing path loss. As a result,

V. CONCLUSION

We consider a downlink mmWave transmission in a cellular-connected UAV network. The desired UAVs are assumed to be served by a terrestrial BS, where the transmit array employs the 3GPP antenna propagation patterns. We also assume that the BS serves the desired UAVs simultaneously using either RSMA or NOMA as the MA scheme. We show that the energy efficiency of either RSMA or NOMA varies non-monotonically with the operation altitude, and RSMA is superior to NOMA in terms of total energy efficiency

REFERENCES

- [1] I. Parvez, A. Rahmati, I. Guvenc, A. I. Sarwat, and H. Dai, "A survey on low latency towards 5G: RAN, core network and caching solutions," *IEEE Commun. Surveys Tuts.*, vol. 20, no. 4, pp. 3098–3130, Fourthquarter 2018.
- [2] A. Rahmati, X. He, I. Guvenc, and H. Dai, "Dynamic mobility-aware interference avoidance for aerial base stations in cognitive radio networks," in *Proc. IEEE INFOCOM*, May 2019.
- [3] M. Mozaffari, A. T. Z. Kasgari, W. Saad, M. Bennis, and M. Debbah, "Beyond 5G with UAVs: Foundations of a 3D wireless cellular network," *IEEE Trans. on Wireless Commun.*, vol. 18, no. 1, pp. 357–372, 2019.
- [4] N. Rupasinghe, Y. Yapici, I. Guvenc, and Y. Kakishima, "Non-orthogonal multiple access for mmWave drone networks with limited feedback," *IEEE Trans. Commun.*, vol. 67, no. 1, pp. 762–777, Jan. 2019.
- [5] N. Rupasinghe, Y. Yapici, I. Guvenc, M. Ghosh, and Y. Kakishima, "Angle feedback for NOMA transmission in mmWave drone networks," *arXiv preprint arXiv:1808.07097*, 2018.
- [6] Y. Mao, B. Clerckx, and V. O. Li, "Rate-splitting multiple access for downlink communication systems: bridging, generalizing, and outperforming SDMA and NOMA," *EURASIP J. on Wireless Commun. and Networking*, vol. 2018, no. 1, p. 133, 2018.
- [7] G. Geraci, A. Garcia-Rodriguez, L. G. Giordano, D. López-Pérez, and E. Björnson, "Understanding UAV cellular communications: From existing networks to massive MIMO," *arXiv preprint arXiv:1804.08489*, 2018.
- [8] 3GPP TR 36.873 v12.4.0, "Technical specification group radio access network; study on 3D channel model for LTE," *Tech. Rep.*, 2013.
- [9] T. S. Rappaport, Y. Xing, G. R. MacCartney, A. F. Molisch, E. Mellios, and J. Zhang, "Overview of millimeter wave communications for fifth-generation (5G) wireless networks—with a focus on propagation models," *IEEE Trans. Antennas Propag.*, vol. 65, no. 12, pp. 6213–6230, Dec. 2017.
- [10] G. Lee, Y. Sung, and J. Seo, "Randomly-directional beamforming in millimeter-wave multiuser MISO downlink," *IEEE Trans. Wireless Commun.*, vol. 15, no. 2, pp. 1086–1100, 2016.
- [11] Z. Ding, P. Fan, and H. V. Poor, "Random beamforming in millimeter-wave NOMA networks," *IEEE access*, vol. 5, pp. 7667–7681, 2017.
- [12] W. Mei and R. Zhang, "Uplink cooperative NOMA for cellular-connected UAV," *arXiv preprint arXiv:1809.03657*, 2018.
- [13] M. Rebato, L. Resteghini, C. Mazzucco, and M. Zorzi, "Study of realistic antenna patterns in 5G mmwave cellular scenarios," *arXiv preprint arXiv:1802.01316*, 2018.
- [14] 3GPP TR 38.901 version 14.0.0, "5G; study on channel model for frequencies from 0.5 to 100 GHz," *Tech. Rep.*, 2017.
- [15] B. Rimoldi and R. Urbanke, "A rate-splitting approach to the Gaussian multiple-access channel," *IEEE Trans. Inf. Theory*, vol. 42, no. 2, pp. 364–375, 1996.
- [16] Y. Mao, B. Clerckx, and V. O. Li, "Energy efficiency of rate-splitting multiple access, and performance benefits over SDMA and NOMA," *arXiv preprint arXiv:1804.08330*, 2018.
- [17] Y. Xu, C. Shen, Z. Ding, X. Sun, S. Yan, G. Zhu, and Z. Zhong, "Joint beamforming and power-splitting control in downlink cooperative SWIPT NOMA systems," *IEEE Trans. Signal Process.*, vol. 65, no. 18, pp. 4874–4886, Sep. 2017.
- [18] M. Grant, S. Boyd, and Y. Ye, "CVX: Matlab software for disciplined convex programming," 2008.
- [19] J. Lofberg, "YALMIP: A toolbox for modeling and optimization in MATLAB," in *Proc. IEEE Int. Symp. on Computer Aided Control Systems Design*, 2004, pp. 284–289.

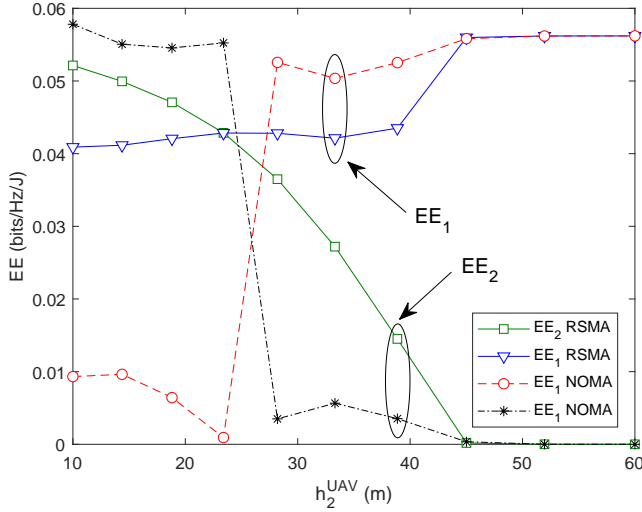


Figure 5: Energy efficiency of each UAV versus the altitude of the 2nd UAV.

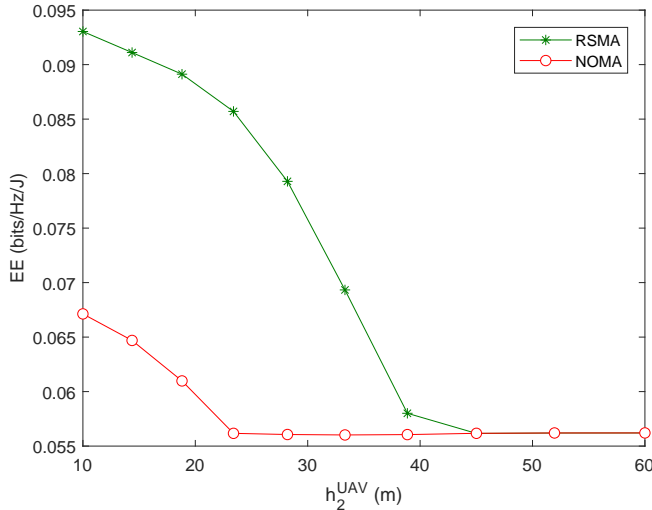


Figure 6: Sum energy efficiency versus the altitude of the 2nd UAV.

the 1st UAV is allocated more power, and its energy efficiency improves as h_2^{UAV} increases. We also observe that although individual energy efficiency of RSMA and NOMA can be superior to one another at certain altitudes, and the sum energy efficiency of RSMA is significantly superior to that of NOMA.

We now change the setting such that the locations of UAVs projected onto the ground are given by the horizontal distances $d_1 = 20\text{m}$ and $d_2 = 50\text{m}$, and angles $\phi_1 = \pi/10$, and $\phi_2 = 2\pi/5$. In addition, altitude of the 1st UAVs is $h_1^{\text{UAV}} = 14.4\text{m}$ with a vertical angle of $\theta_1 = 4\pi/9$, and altitude of 2nd UAV is varying such that $h_2^{\text{UAV}} \in [0, 60]\text{m}$, as before. The respective individual and sum energy efficiency results are depicted in Fig. 5 and Fig. 6, respectively. We observe that the performance gap of RSMA and NOMA appears to be more significant in favor of RSMA in this particular setting (as compared to that of Fig. 4).